

UNCLASSIFIED

AD 666 525

DROP BREAKUP BY AIRSTREAM IMPACT

James E. Nicholson

Mithras, Incorporated
Cambridge, Massachusetts

1968

Processed for . . .

DEFENSE DOCUMENTATION CENTER
DEFENSE SUPPLY AGENCY



U. S. DEPARTMENT OF COMMERCE / NATIONAL BUREAU OF STANDARDS / INSTITUTE FOR APPLIED TECHNOLOGY

UNCLASSIFIED

1. INTRODUCTION

Rain droplets which enter the flow field surrounding aircraft and missiles will be subjected to an impulsively applied aerodynamic pressure which is capable of disintegrating the droplets. The objective of this paper is to examine in detail the problem of drop breakup by airstream impact.

When a drop of liquid is suddenly exposed to an airstream, various competing forces determine whether the drop will be broken up and, if so, how long the process will take. The forces which act to tear apart the droplet scale approximately with dynamic pressure, $1/2 \rho V^2$. The tendency to distort the drop shape is resisted by inertia forces, surface tension forces, and, to a lesser extent, by viscous forces.

Although many variables ultimately affect drop breakup, the most important in the discussions which follow is the Weber number;

$$W_e = \frac{\rho_a V^2 d}{2 \sigma} \quad (1)$$

which represents the ratio of the pressure to surface tension forces. Whether or not a droplet is broken up is determined by the magnitude of the Weber number. Lane², Hanson, Domich and Adams³ and others^{4, 5} have made detailed measurements of the critical Weber number required for droplet breakup. These values vary from about 4 to 13 and correspond to velocities of 40 to 200 feet per second at sea level for drop diameters of 1 mm to 2 mm which are representative of the size found in a typical rain storm.

More recently the problem of droplet breakup has been examined at conditions which correspond more closely to flight in the atmosphere. Engel⁶ has conducted shock tube studies in which the shock front speeds corresponding to Mach numbers of 1.3, 1.5 and 1.7 were achieved at an ambient pressure of one atmosphere. In previous drop breakup studies it had been observed that the droplets could breakup by vibrating with increasing amplitude ($W_e \approx (W_e)_{crit.}$) or the droplets would inflate like a parachute until they burst in the center ($W_e > (W_e)_{crit.}$). Engel found that, in contrast to these modes, droplets under severe impact loading ($W_e \gg (W_e)_{crit.}$) would flatten out into a disc shape where material would be stripped from the edge. In general the third type of breakup observed by Engel⁶ will be the main concern of this paper.

2. SCALING LAWS FOR DROPLET BREAKUP BY HIGH SPEED AIRSTREAM IMPACT

In a complete analysis of droplet breakup a number of variables must be considered — surface tension, inertia, viscous forces, Mach number and two Reynolds numbers. A generalized breakup function may be written

$$\bar{t} = f(\bar{\rho}, Re_a, We, M, Re_w) \quad (2)$$

By examining the order of magnitude of the terms involved⁷ and eliminating higher order effects the drop breakup function is reduced to

$$\bar{t}_b = \frac{t_b V}{d} = f\left(\frac{\rho_l}{\rho_a}, M\right) \quad (3)$$

where ρ_l/ρ_a is the ratio of droplet density to air density and M is the relative Mach number.

The Mach number, M , represents the influence of compressibility on reduced breakup time. Since the droplet starts out as a sphere one would expect the drag coefficient of a droplet to be similar to that of a solid sphere (Figure 1). At low subsonic speeds the effect of M on pressure distribution is small. However, at transonic speeds Mach number begins to play a role through changes in the pressure distribution on the droplet. The pressure distribution again becomes invariant at supersonic speeds and no further Mach number dependence is expected. No data are available to substantiate these conjectures and subject to confirmation, the Mach number of the impacting airstream will be assumed to play a minor role in the breakup process.

The governing relations for droplet breakup are derived in the following analysis. The pressure gradient across the droplet is proportional to $2\rho_a V^2/d$. Newton's third law for droplet distortion, δ may be written as

$$\delta = \frac{2\rho_a}{\rho_l} \frac{V^2}{d} \quad (4)$$

where δ is defined in Figure 2. Neglecting in this simple model any change in pressure gradient as the drop distorts, the distortion as a function of time may be written as

$$\delta = \frac{\rho_a}{\rho_l} \frac{V^2}{d} t^2 \quad (5)$$

The relative distortion is

$$\epsilon = \frac{\delta}{d} = \frac{P_a}{\rho_l} \left(\frac{V_t}{d} \right)^2 \quad (6)$$

Breakup is assumed to occur when ϵ reaches a critical value which must be determined by experiment.

The expression for droplet breakup can be rewritten in familiar aeronautical parameters

$$\frac{t_b}{d} = \left(\frac{\epsilon \rho_l}{2} \right)^{1/2} q^{-1/2} = k q^{-1/2} \quad (7)$$

where q is the impact pressure. For water droplet breakup

$$k = 6.85 \sqrt{\epsilon} \quad (8)$$

where ϵ is dimensionless and k is expressed in $(\text{psi})^{1/2}$ seconds per inch.

3. SHOCK TUBE MEASUREMENTS OF DROP BREAKUP

A series of experiments were run in the MIT 8 by 24 in. shock tube to obtain qualitative data on drop breakup under conditions relevant to high speed flight through rain⁷. The objectives of these experiments were to confirm, if possible, the scaling laws for high speed impact developed in the previous section and to obtain the value of the empirical constant in Equation (7). Before these objectives could be realized, an unambiguous definition of the completion of the breakup process had to be established so that the interval, t_b , could be measured. This point has been neglected by previous investigators whose interest lay mainly in low speed impact and determination of the critical parameters for drop breakup.

3.1 Description of Experiments

The shock tube in the MIT Aeroelastic and Structures Research Laboratory has been described elsewhere (Reference 8). It is driven by cold air or helium and can generate airspeeds behind the shockwave of up to about 3000 fps. The initial pressure may be reduced to about 0.5 psia by vacuum pumps.

During these tests, drops with a nominal diameter of 1.5 mm were introduced into the shock tube by dripping water from a 0.016 in. hypodermic tubing mounted in the top of the shock tube. The firing of the shock tube was synchronized with the start of a Fastax camera which photographed the breakup process at about 13,000 frames per second. The arrival of the shock wave at the drop was determined by an event marker and the frame rate was measured with a 120 cps timing light. A schematic of the experimental setup is shown in Figure 3.

The test program consisted of 32 runs, covering the 6 test conditions listed in Table I. Initially the camera covered a fairly small field of view to obtain enough magnification to allow a measurement of drop size. Later, the same conditions were repeated with a large field of view to follow the breakup process to completion.

A typical sequence of photographs obtained with the small field of view is shown in Figure 4. The individual frames have been aligned with a fixed reference mark in the shock tube to show the motion of the drop as well as its breakup as expected. These pictures indicate that the breakup process was of the third type discussed in the Introduction. The drops were first deformed into discs normal to the flow and then droplets were stripped from the exposed edges.

A typical series of drop displacement data is shown in Figure 5. Note that the data, taken at the same impact pressure, shows no sign of influence of local Mach number on droplet drag.

3.2 Criterion for Breakup Completion

The breakup of a drop begins when droplets are sheared from the edge of the drop core by aerodynamic forces. This process can be reasonably considered complete when the remaining core is not much larger than the fragments being stripped off.

Since a steady light source was used to take the Fastax pictures, the exposure time was set by the camera framing rate and was much too long to resolve moving drops. However, an indication of the size of the shrinking drop may be obtained by examining its motion. The drop's location is of course at the leading edge of the droplet cloud seen in Figure 4. Figure 6 shows a curve of drop displacement versus time for a typical run. Also shown is a curve of drop velocity versus time obtained by numerical differentiation of the displacement data. The sharp break in the slope of the velocity curve was observed in every run, and indicates a sudden increase in the drop acceleration and hence in the area/volume ratio. At this point, the remaining core of the original drop apparently shatters into a number of much smaller drops. For practical purposes, the breakup process is complete and a value of the breakup time, t_b , may be read off the curve.

This definition of t_b was adopted for all data, and values were read off curves similar to the one illustrated in Figure 6. The definition is new and introduced a quantitative criterion for the completion of breakup where

previous investigators had relied on subjective interpretation of photographs.

3.3 Results of Shock Tube Measurements

The defined time to breakup a droplet was normalized by droplet diameter and plotted in Figure 7 versus dynamic pressure, $q = 1/2 \rho_a V^2$. With logarithmic scales on both axes, Equation (7) is represented by a straight line with a slope of $-1/2$; this line fits the data quite well.

The equation of the line shown may be written

$$t_b/d = 23.9 q^{-1/2} \quad (9)$$

where

- t_b = breakup time in ms
- d = drop diameter in inches
- q = dynamic pressure in psia

The corresponding value of the empirical constant

$$\epsilon = \frac{2q}{\rho_l} \left(\frac{t_b}{d} \right)^2 \quad (10)$$

is $\epsilon = 12$ which is in excellent agreement with the range of values between 10 and 15 previously reported for jets by Clark⁹.

Some data from previous experiments have also been plotted in Figure 7. Quite good agreement with the present results is obtained in spite of possible differences in the definition of the completion of the breakup process.

The shock tube results may also be used to define a breakup distance (i. e., is the displacement of the drop during the breakup process). Figure 6 shows that the drop acceleration is approximately constant during the breakup process, so that the displacement at drop break-up may be written

$$S_b = \frac{1}{2} a t_b^2 \quad (11)$$

The acceleration, a , is equal to the ratio of the aerodynamic drag on the drop to its mass,

$$\begin{aligned} a &= \frac{D}{M} \\ &= \frac{3C_D}{4} \frac{\rho_a V^2}{\rho_l d} \end{aligned} \quad (12)$$

where C_D is the drag coefficient. Therefore,

$$\begin{aligned} S_b &= \frac{3C_D}{8} \frac{\rho_a V^2}{\rho_l} \frac{t_b^2}{d^2} d \\ &= \frac{3}{8} \epsilon C_D d \end{aligned} \quad (13)$$

where ϵ is the empirical constant introduced previously. The drag coefficient, C_D , on the distorted drop is not known but may be presumed invariant. This simple analysis thus predicts that S_b/d should be constant.

Figure 8 shows the values of S_b/d measured in the shock tube experiments versus the impact dynamic pressure. The predicted invariance is confirmed within the experimental accuracy and the best fit to the data is

$$S_b/d = 12 \quad (14)$$

This value is independent of the velocity or density of the air, although a possible variation with the density of the liquid cannot be ruled out since only water drops were used.

Final droplet sizes were deduced by measuring the acceleration of the shattered droplets after droplet breakup. These droplets were assumed to behave as spheres and the drag was derived from the data of Figure 1. The Weber number of the flow was computed based on derived droplet diameter and the data has been plotted in Figure 9. Also plotted is the basic data of Lane², Hanson³ et al. and Ingebo¹². It is interesting to note that final droplet sizes are on the order of 50 microns to 200 microns and the critical Weber number for obtaining these droplets is about one order of magnitude greater than that for initial breaking of droplets.

3.4 Transformation of Breakup Time to Breakup Distance

Information is now available on the time to breakup droplets and the displacement of droplets during the breakup process. The length of dead air required to breakup droplets in flight can be calculated by performing a suitable transformation of coordinates. With reference to Figure 10, we shall assume that a 'dead air' zone can be constructed so as to move with a vehicle. The air between the bow of a vehicle and its shock wave moves at approximately the vehicle speed.

The leading edge of the flow discontinuity travels a distance $V_2 t_b$ in the time required to breakup a droplet. However the droplet has meanwhile been displaced by the impacting flow a distance S_b . The minimum standoff distance required to break up a droplet is thus

$$S^* = V_2 t_b - S_b \quad (15)$$

By substituting Equations 9 and 14 into 15 and equating V_2 with V_∞ we get

$$\frac{S^*}{d_0} = 0.286 \frac{V_\infty}{(q_2)^{1/2}} - 12.1 \quad (16)$$

This function has been plotted in Figure 11 versus Mach number for several altitudes assuming that ram pressure is available to break up the droplets. In supersonic flight ram pressure is equal to pitot pressure and in subsonic flight ram pressure was assumed to be equal to stagnation pressure.

4. DROP BREAKUP BY "DEAD AIR" FLOWS

In this section we shall examine some of the mechanisms for creating a "dead air" flow, and summarize available data on drop breakup by "dead air" flows.

4.1 Blunt Body Flows

A limited number of mechanisms will provide a zone of air which travels along with a vehicle. For a blunt body the air between the shock wave and the body moves at approximately the vehicle speed. This flow creates a pressure which is approximately equal to pitot pressure and is capable of shattering droplets which cross the shock wave. The shock wave stand-off distance is a function of Mach number, as shown in Figure 12, and is generally expressed as a fraction of the body diameter.

Note that the shock wave moves in closer to the body as the free stream Mach number is increased. Unfortunately no data is available on blunt body rain erosion protection by shock stand-off.

4.2 Impact Tube

Recently experiments in droplet breakup by dead air flows have been reported by Jenkins¹ and Nicholson and Figler⁷. In Jenkins¹ experiment a hollow projectile was fired at a droplet suspended on a web. The hollow cylinder was opened at the front end and closed in the rear so that the moving flow was trapped. The rear of the projectile was constructed from transparent material. Breakup of a 2 mm water droplet inside of the hollow projectile was photographed while the projectile moved at 560 feet per second. The droplet was nearly broken up at a distance of 2.4 inches from the entrance of the cylinder. The impact pressure of the trapped flow is computed to be 18 psi.

In the experiment reported by Nicholson and Figler⁷ an open ended cylinder was mounted on end in the supersonic tunnel of the Massachusetts Institute of Technology Gas Turbine Laboratory. A jet of water was fired downstream at brass and lead targets mounted at the base of the open ended cylinder. A picture of the setup is shown in Figure 13. The velocity of the water jet was closely matched to the free stream wind tunnel speed so as to simulate flight in the rain. The length of the plexiglass tube was varied from 0 to 6 inches so as to determine that length which would break up the droplets prior to damaging the targets.

Droplet sizes and jet velocities were measured with a high speed photographic system consisting of two cameras each with a flash unit and an electronic time delay circuit, and actuated by a photoelectric triggering circuit. The majority of the droplets measured for photographs were 2 mm diameter or less. The length of cylinder required to protect the targets from appreciable damage were on the order of 3 to 6 inches. At best only a bracket on drop breakup length could be established with this technique. These measurements were taken at an equivalent flight altitude of 48,000 ft at Mach number 2. These conditions correspond to an impact pressure of 10.6 psi.

4.3 Spiked Body Flow

Of all the simulation techniques available, the rocket sled test alone bears the ability to test full scale models at realistic flight velocities. Nicholson and Figler⁷ have reported drop breakup tests on a spiked flat aluminum plate which was run at the Air Force Missile Development Center Test Track Division at Holloman Air Force Base, New Mexico (Reference 11).

The high speed track at Holloman is 35,000 ft long with a 6000 ft run of simulated rain generated by mounting precisely controlled nozzles in a double row along the test track. The rain rate was 5 in. per hour with a nominal drop size of 1.5 mm.

The model consisted simply of a 7 in. long steel spike mounted at the center of a 6 in. diameter aluminum faceplate. The model was mounted on a Sandia Corporation rocket sled boosted by two stages of propulsion to approximately 3000 fps; at this speed a small sustainer engine was employed to maintain velocity through the rain field. The average velocity of the model through the rain field was 3035 fps + 10 fps. These conditions correspond to an impact pressure of 102 psi.

The spike-induced flow pattern is shown schematically in Figure 14. The major feature of the flow field is the dead-air region bounded at the base by the body face and at the sides by a shear layer. This free shear layer begins where the boundary layer on the spike separates because of pressure rise at the dead-air region, and ends at or near the edge of the body face where it re-attaches to form a conventional boundary layer. Velocities in the separated flow or dead-air region are much smaller than in the free stream, and the pressure is nearly constant. Therefore, this region assumes a conical shape with the cone axis aligned with the flow. At the re-attachment point, some of the boundary layer air, with significant velocity, is turned into the separated region and causes the low speed circulation in the region.

4.3.1 Interaction of Rain Drops with the Spike-Induced Flow Pattern

The spike-induced flow ahead of the faceplate subjects any rain-drop it encounters to the impact of an airstream moving at the vehicle speed. This impact is actually applied in two steps, the first and smallest at the shockwave and the second at the mixing layer. At moderate supersonic flight speeds, the airstream left by a drop after the shockwave passes it is only about 10 percent of the vehicle speed. Only after the drop becomes immersed in the conical region of separated flow does it feel the full impact of an airstream moving at the flight speed of the vehicle.

This impulsively applied airstream has two effects on raindrops, which greatly reduce the raindrop capability to erode the faceplate surface. First, the air stream shatters most drops into much smaller droplets, and second, it accelerates unshattered drops and drop fragments to some fraction of the vehicle velocity. This reduces the relative velocity at impact and hence, the amount of erosion at the faceplate. Most easily accelerated are the smaller drops and drop fragments. A reasonable hypothesis is that none of the water originally present in drops can do any damage when shattered. As for erosion damage, only the liquid water content of drops too large to be shattered need be counted. Even these drops are accelerated and lose some of their mass before impacting the radome so the damage they can do is less than the damage if they impacted at the vehicle speed.

4.3.2 Measurement of Breakup Distance with the Spike-Protected Faceplate

Figure 15 is a post-test photograph of the spike-protected faceplate. Since the decision to conduct this test was made during a more comprehensive test program, this configuration was generated by altering another test model. Four threaded holes and an annular slot filled with fiberglass are shown in the photograph.

After the test, a series of measurements was made to determine the variation of surface roughness across the plate. The results are plotted in Figure 16 in terms of the standard deviation of surface pit depth. Surface roughness varied from less than 0.0002 at a radius of 7/8 in. to a maximum of 0.0048 at a radius of 2-3/8 in. Surface roughness decreases beyond this radius to approximately 0.0030, apparently because the drops peened the surface. At the rim of the plate, surface roughness is 0.0043. No measurements were made of surface damage to the 0.25 in. thick fiberglass ring to the plate. The abscissa of Figure 16 represents the breakup distance available between the dividing streamline in the mixing layer and the surface of the plate which varies linearly from zero at the rim to 7 in. at the center, corresponding to the physical spike length.

The increase in surface roughness in going from the center to the rim of the plate is consistent with the drop breakup model presented above. Drops of critical diameter, d^* , are completely broken up near the center and drops above this diameter are reduced in size and may cause damage to the model. If all drops within a given rainstorm are below the critical diameter, d^* , no damage can occur to the model. In fact there is a cut-off diameter, d , larger than d^* which will be sufficiently reduced in size so as not to cause significant damage to a given material target. The criterion for significant damage depends entirely on the tolerable damage limit which a given situation can withstand.

5. COMPARISON OF THEORY AND DATA

The theory of section 3 has been developed to predict the length of dead air required to protect a body in flight. Using Equation (16) it is possible to compute a map of distance required to breakup droplets by aerodynamic impact versus impact pressure for a series of trajectories in the atmosphere. These values have been computed for sea level, and 50,000 feet for breakup of various size droplets and plotted in Figure 17.

The available data on drop breakup has been plotted simultaneously in Figure 17. The rocket sled measurements, taken at 4,000 feet elevation are to be compared to the sea level curves constructed at 1 mm, 2 mm and 4 mm. Note that the bound on drop breakup length was considered to extend from 3 to 4 inches at an impact pressure of 102 psi. Since the mean drop diameter at the AFMDC Test Track is 1.5 mm, there is excellent agreement between the rocket sled results and theory.

The drop breakup measurement obtained by Jenkins¹ in the laboratory is to be compared to the sea level predictions shown in Figure 17. In section 3.2 of this study the time to breakup a droplet was defined as the point where there is a sudden acceleration of the leading edge of the droplet. We note from Figure 9 that the droplet sizes which have been deduced by this acceleration criterion are on the order of 50 microns to 200 microns. Jenkins definition of drop breakup is, "Complete disintegration has been arbitrarily taken to be the condition where no droplets greater than 150 microns are collected." Thus the measurement of drop breakup length derived from Jenkins data is probably consistent with the definition of drop breakup suggested herein. The agreement between theory and data for the 2 mm droplet is excellent.

The wind tunnel measurement of drop breakup distance, at an equivalent altitude of 48,000 feet, has been plotted in Figure 17. On a blunt faced cylinder (Figure 12) at a free stream Mach number of 2 the shock wave stands off 0.45 body diameters ahead of the cylinder. For the 1.75 inch diameter cylinder the shock wave will stand off .83 inches. Thus the distance required to diminish the rain gun droplets such that they did no damage to the targets was 3.83 to 6.83 inches.

The longest length required to protect the wind tunnel targets, 6.83 inches corresponds to complete breakup of 1 mm droplets. One must conclude that those droplets in the jet which were larger than one millimeter were reduced in mass and altered in cross section such that the impact pressure of the resultant fragments was insufficient to do damage.

6. CONCLUSIONS

1. Scaling laws for water droplet breakup have been derived and verified by shock tube data. Data is correlated by the relation

$$\left(\frac{p_a}{p_l}\right) \left(\frac{v_t}{d}\right)^2 = \epsilon$$

where the constant ϵ is determined from this experiment to be 12.0. These measurements are in agreement with previous data.

2. The distance required to break up a droplet by a moving 'dead air' zone is derived as

$$\frac{s^*}{d_0} = 0.286 \frac{V_\infty}{q_2^{1/2}} - 12.1$$

This relation has been compared to measurements by the author and others and found to be in excellent agreement. At supersonic speeds the above relation approaches a constant value which is a function only of altitude - increasing with increasing altitude.

3. Drops which are broken up by aerodynamic impact result in droplets which, based on shock tube data, are in the size range from 50 microns to 200 microns diameter. Complete breakup of drops by aerodynamic impact overestimates the amount of dead air separation required to protect a given material from rain erosion. Based on the wind tunnel and rocket sled data this overestimation is probably a factor of two.

TABLE I. Summary of Shock Tube Test Conditions

<u>Driver Pressure (psia)</u>	<u>Driven Pressure (psia)</u>	<u>Driver Gas</u>	<u>V_s (fps)</u>	<u>q₂ (psia)</u>	<u>M₂</u>	<u>Drop Size (inches)</u>
30	1.50	Air	2040	2.67	.839	.060-.070
60	2.90	Air	2050	5.35	.839	.068-.078
120	6.0	Air	2040	10.7	.839	.071
141	2.98	Air	2400	10.5	1.06	.070*
38	1.0	He	3130	10.5	1.32	.070*
103	2.8	He	3080	28.4	1.32	.070*

* Average drop size assumed. Field of view too large to measure drop diameter accurately.

REFERENCES

1. Jenkins, D. C., "Disintegration of Raindrops by Shockwaves Ahead of Conical Bodies," *Philosophical Transactions of Royal Society of London*, Vol. 260, p 153, 28 July 1966.
2. Lane, W. R., Shatter of Drops in Streams of Air, *Industrial and Engineering Chemistry*, Vol. 43, No. 6, pp 1312-1317, 1951.
3. Hanson, A. R., Domich, E. G. and Adams, H. S., An Experimental Investigation of Impact and Shock-Wave Breakup of Liquid Drops, Final Report T 8831, University of Minnesota, November, 1955.
4. Rupe, J. H., A Technique for the Investigation of Spray Characteristics of Constant Flow Nozzles, Part I, Paper Presented at Conference on Fuel Sprays, University of Michigan, March 1949.
5. Gordon, G. D., Mechanism and Speed of Breakup of Drops, *Journal of Applied Physics*, Vol. 30, No. 11 November 1959.
6. Engel, O. G., Fragmentation of Waterdrops in the Zone Behind an Air Shock, *Journal of Research of the National Bureau of Standards*, Vol. 60, No. 3, Research Paper 2842 March 1958.
7. Nicholson, J. E. and Figler, B. D., "Complementary Aerodynamic Test Techniques for Rain Erosion Alleviation Studies," AIAA Paper 66-766, September 1963.
8. Ruetenik, J. Ray and Witmer, Emmett, A., Transient Aerodynamics of Two-Dimensional Air Foils, Part I, MIT Aircraft Lab., August 1956, WADC Tech Report 54-368, Part I.
9. Clark, B. J., Breakup of a Liquid Jet in a Transfer of Gas, NASA TN D-2424, August 1964.
10. Wolfe, H. E. and Anderson, W. H., Kinetics, Mechanism and Resultant Droplet Sizes of the Aerodynamic Breakup of Liquid Drops, Aerojet-General Corp., Report 0395-04 (18), SP, April 1964.
11. Holloman Track Capabilities, Technical Documentary Report No. MDC-TDR-62-9, September 1962.
12. Ingebo, R. D., and Foster, H. H., "Drop-Size Distribution for Crosscurrent Breakup of Liquid Jets in Airstreams." NACA TN 4087, 1957.

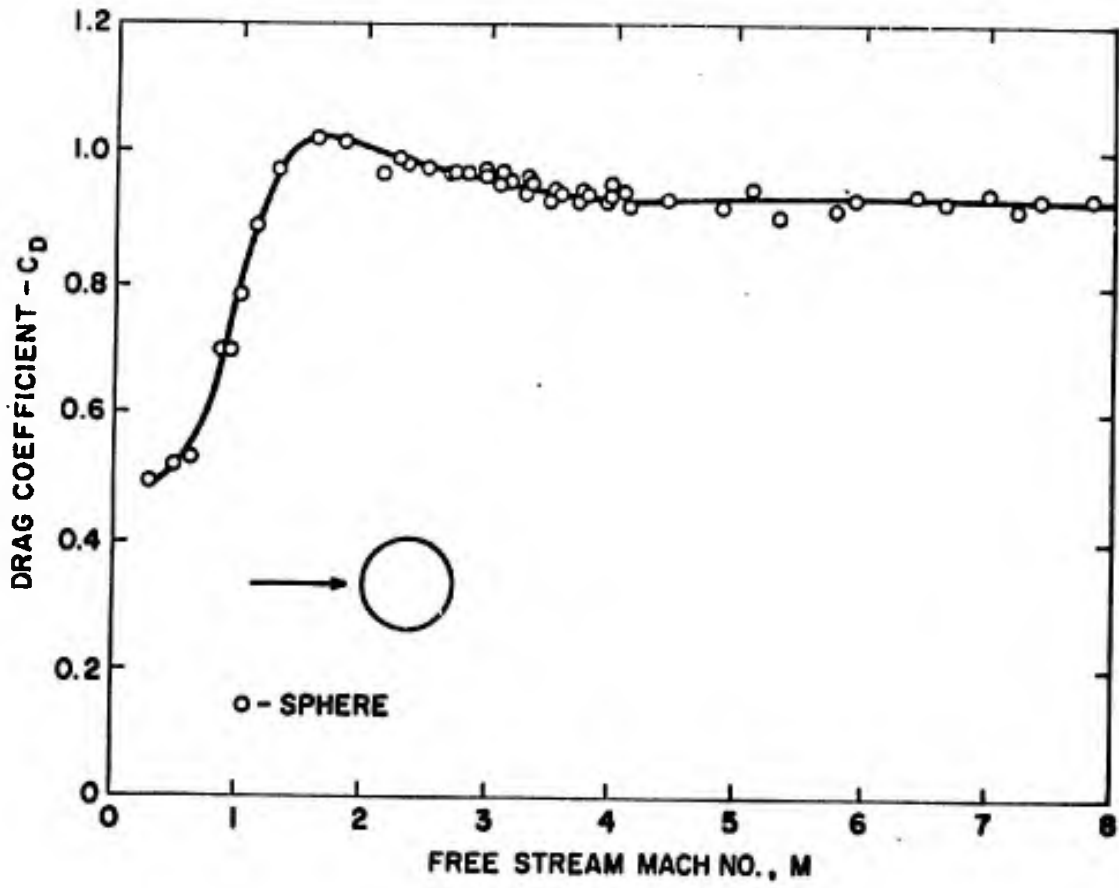


Figure 1. Drag Coefficient of a Sphere

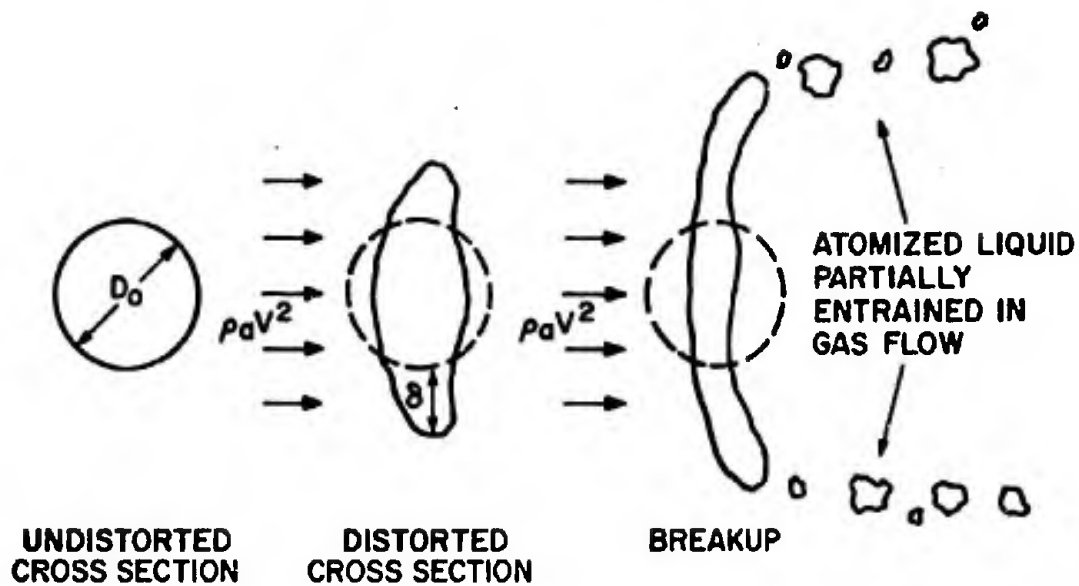


Figure 2. Model of Drop Breakup

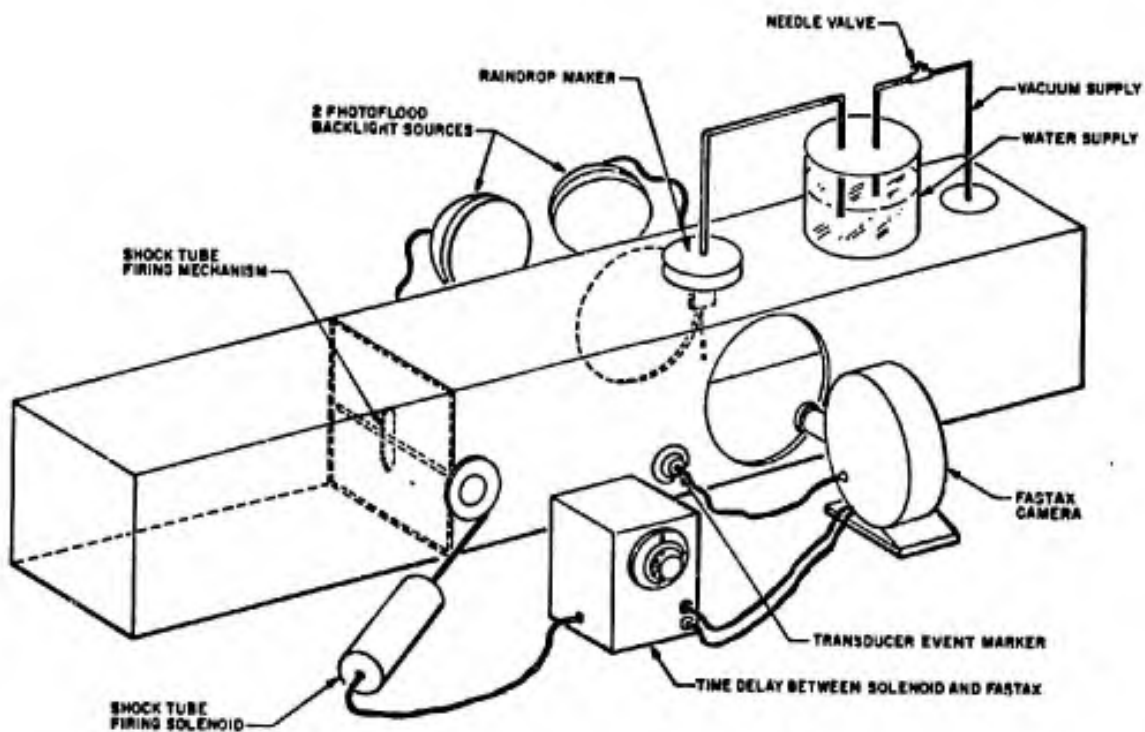


Figure 3. Schematic of Shock Tube Experiment

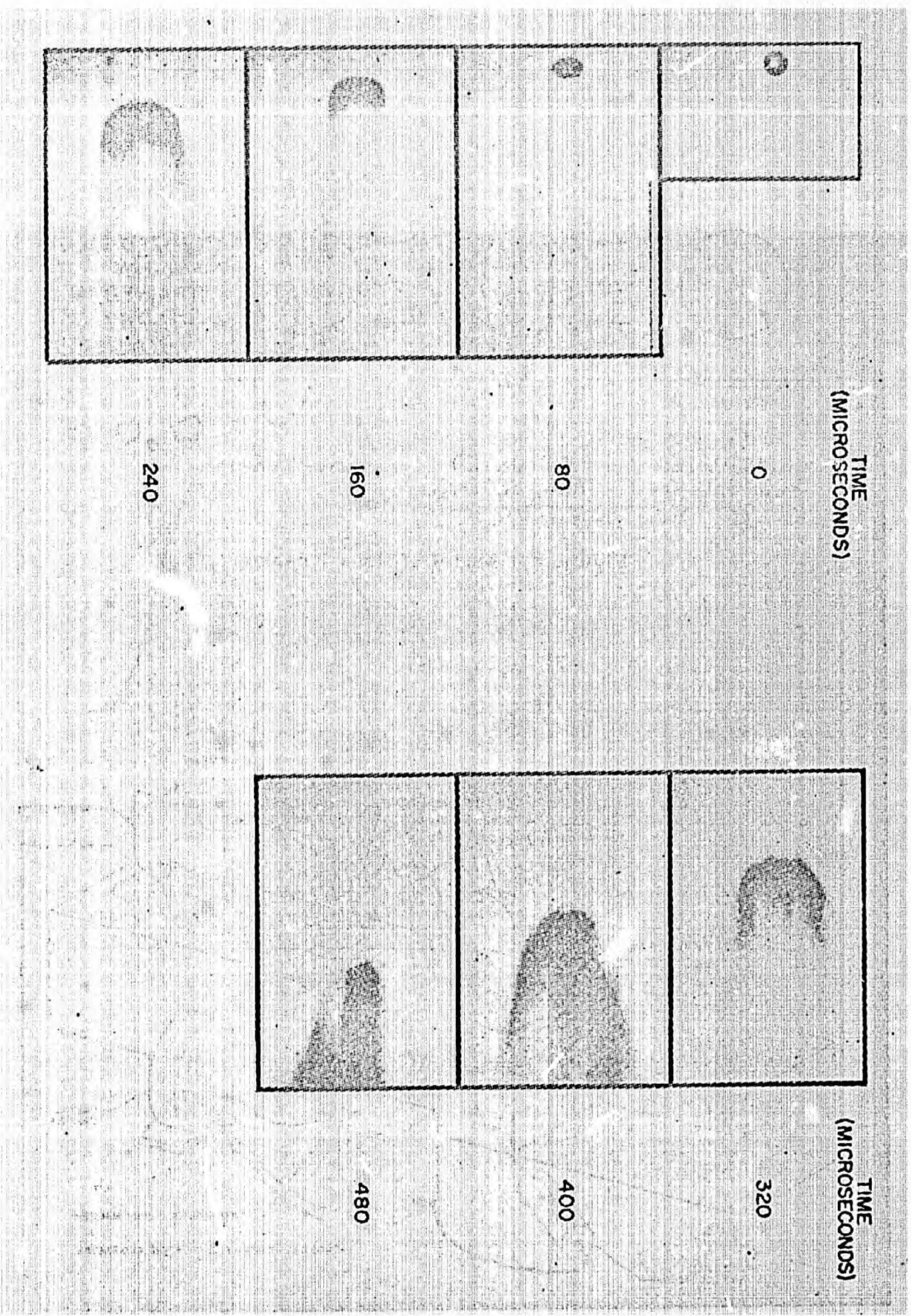
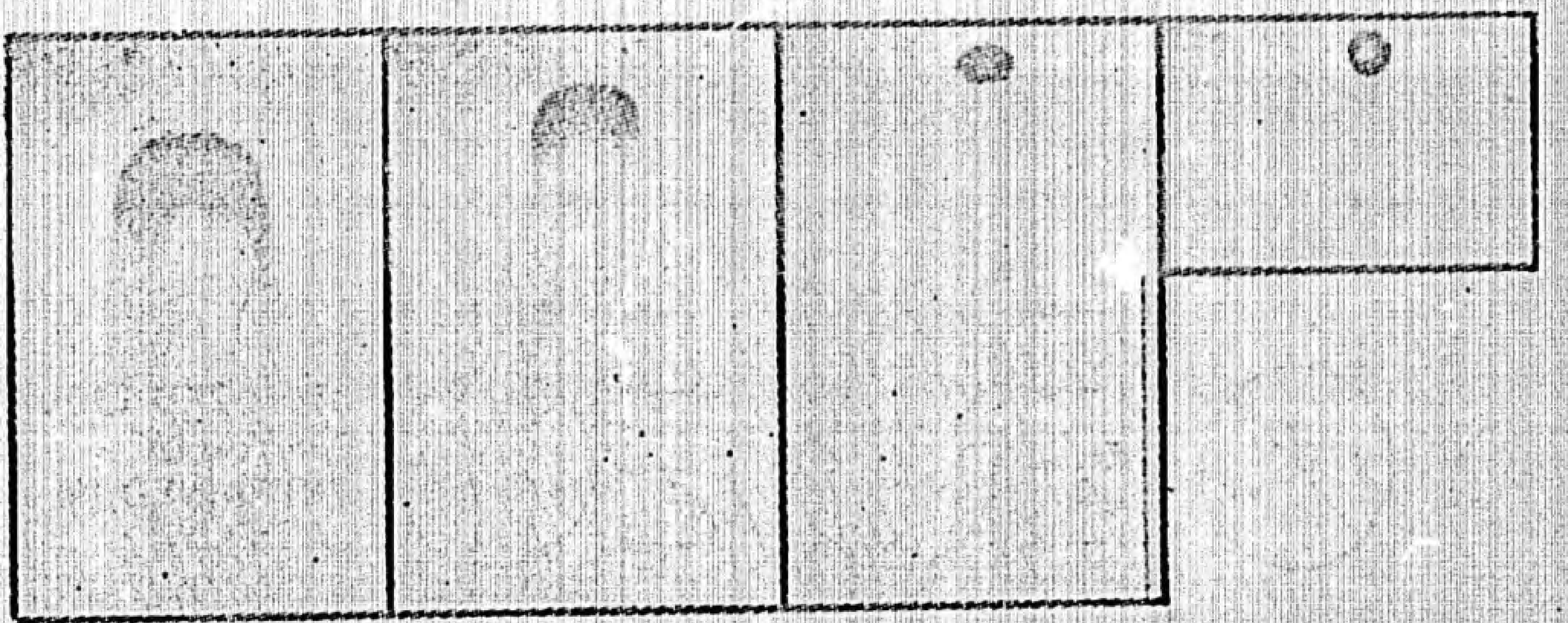


Figure 4. Sequential Photographs of Drop Breakup



TIME
(MICROSECONDS)

0

80

160

240



TIME
(MICROSECONDS)

320

400

480

Figure 4. Sequential Photographs of Drop Breakup

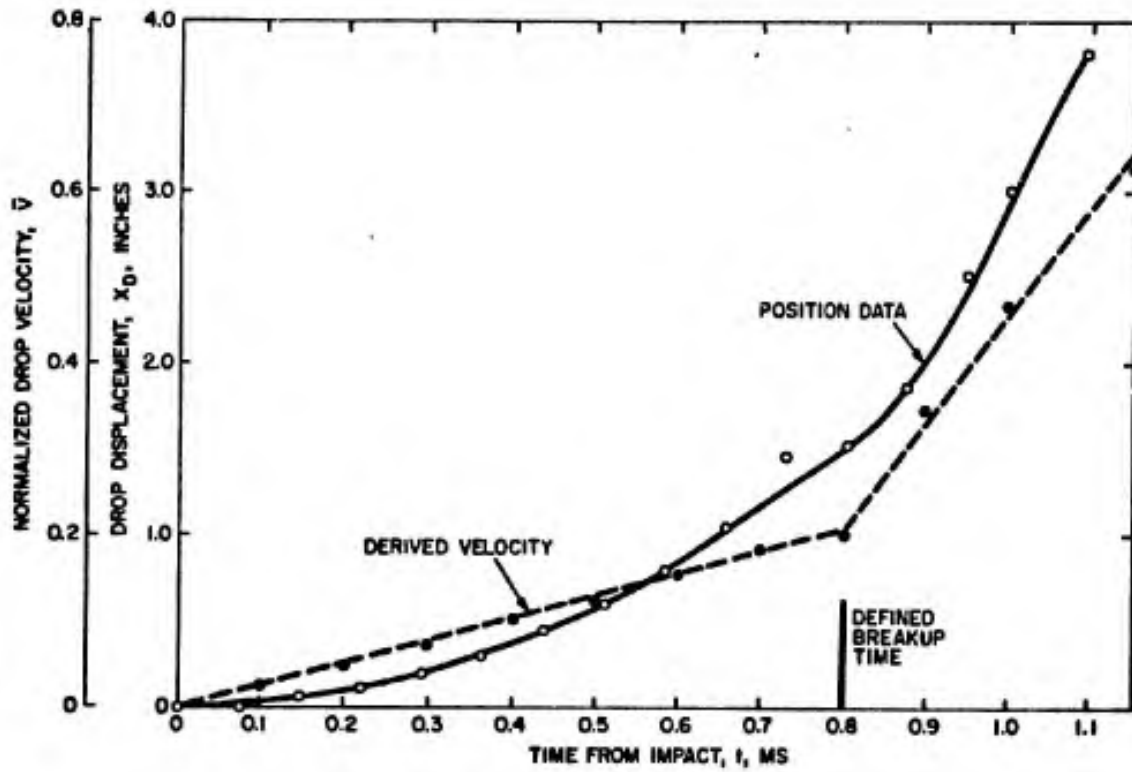


Figure 6. Time History of Drop Displacement and Velocity

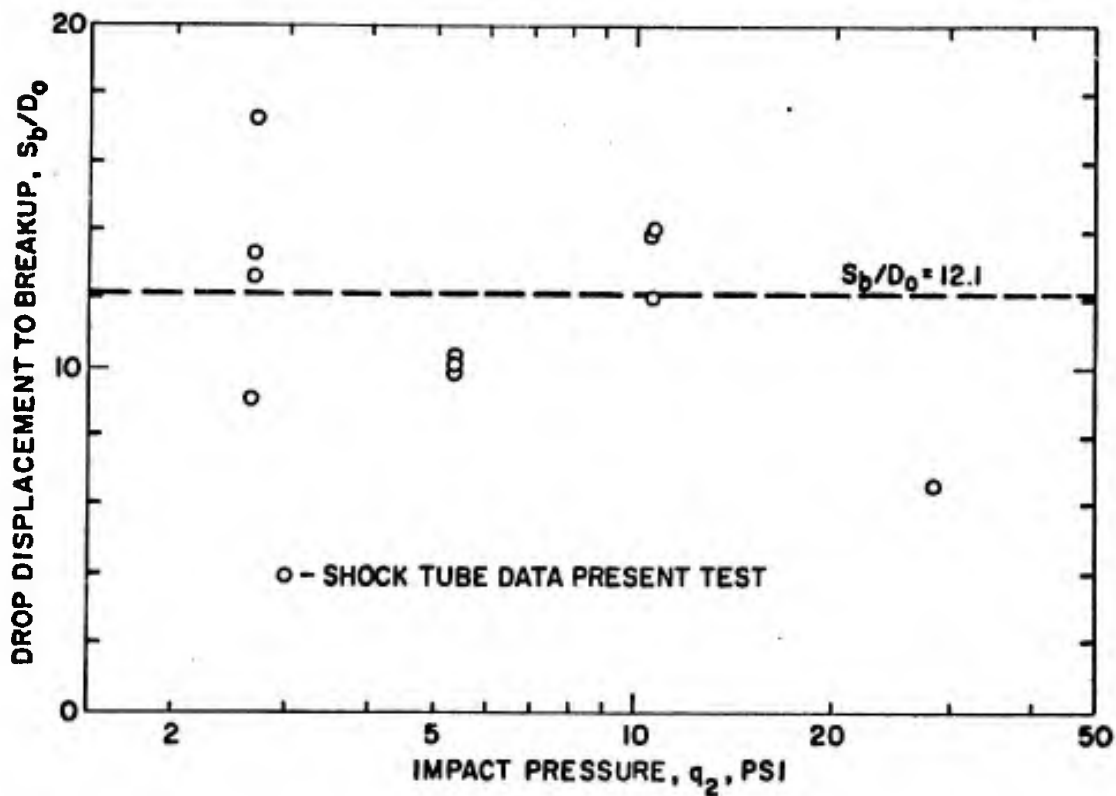


Figure 8. Drop Displacement to Breakup versus Impact Pressure

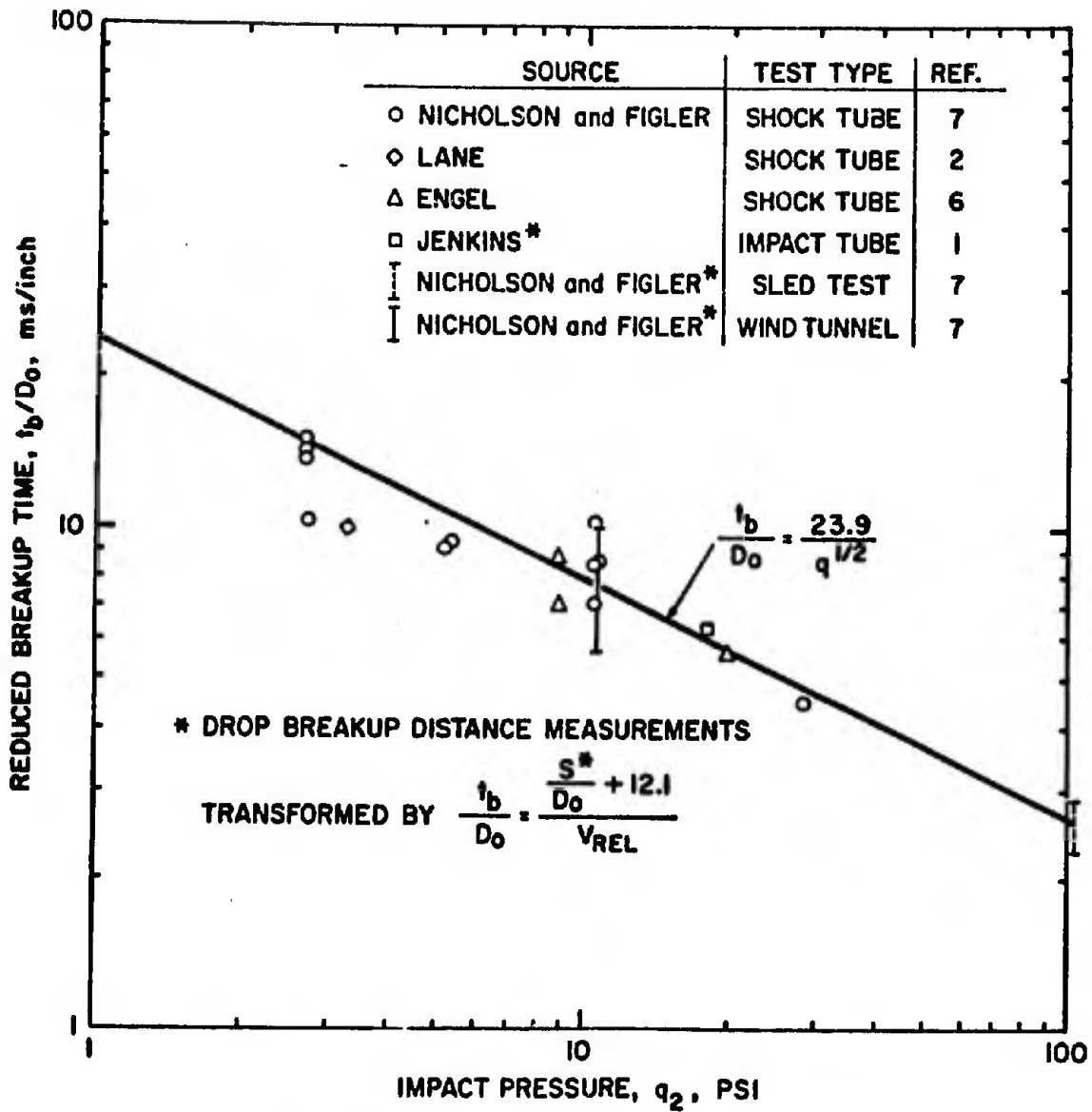


Figure 7. Summary Plot of Drop Breakup Time versus Impact Pressure

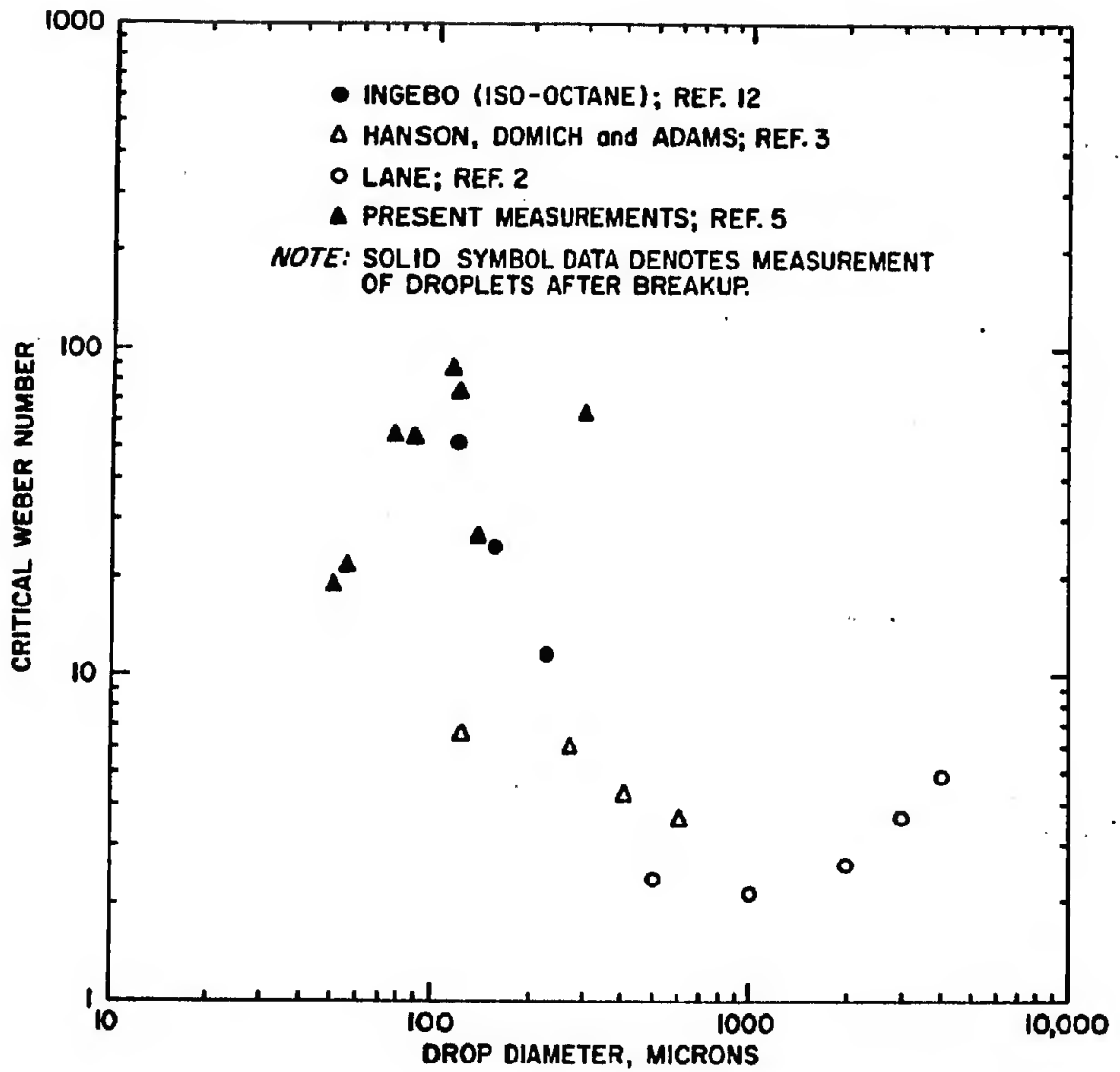


Figure 9. Terminal Droplet Size versus Weber Number for Drop Breakup by Airstream Impact

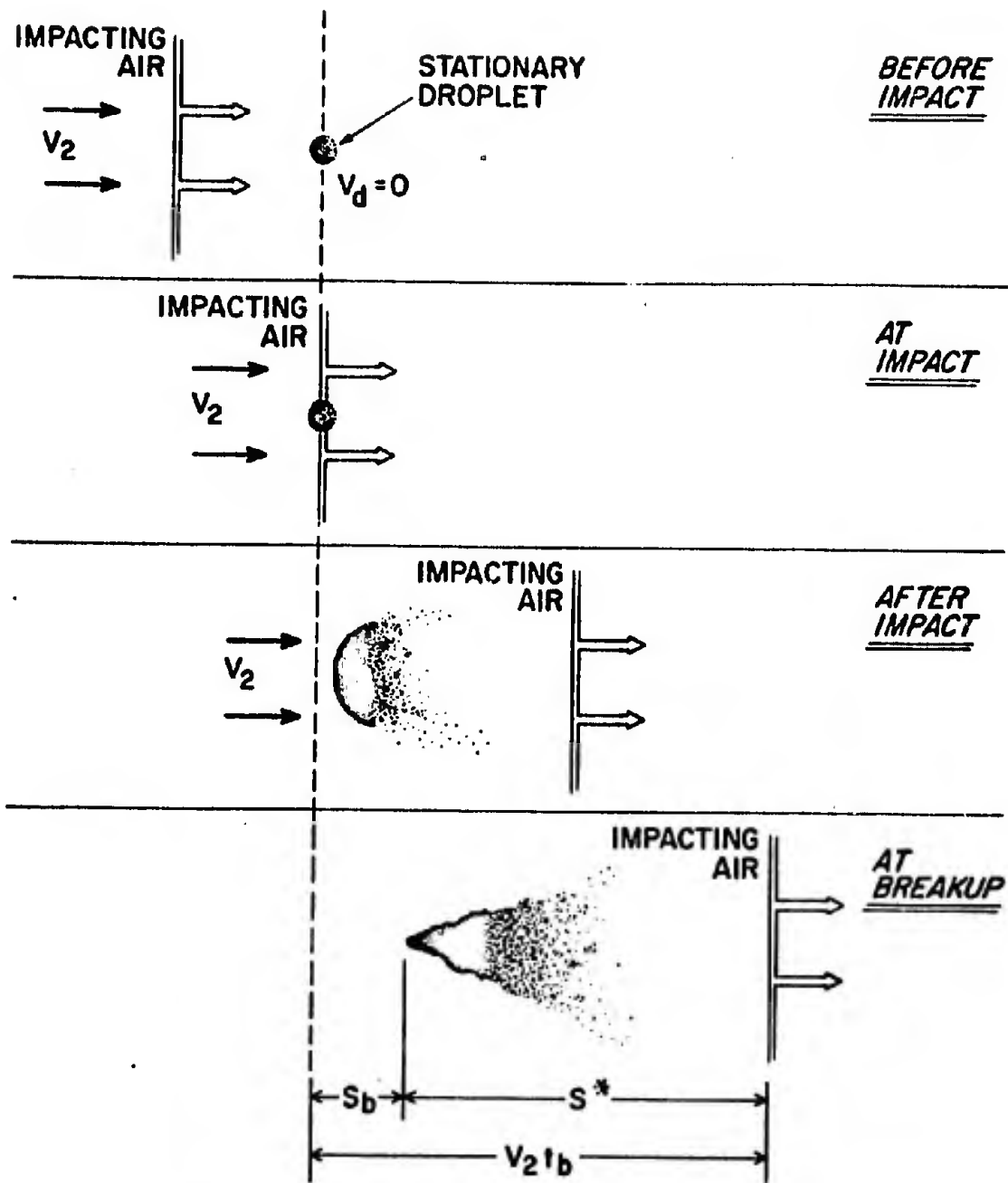


Figure 10. Schematic Time History of Drop Displacement During Breakup

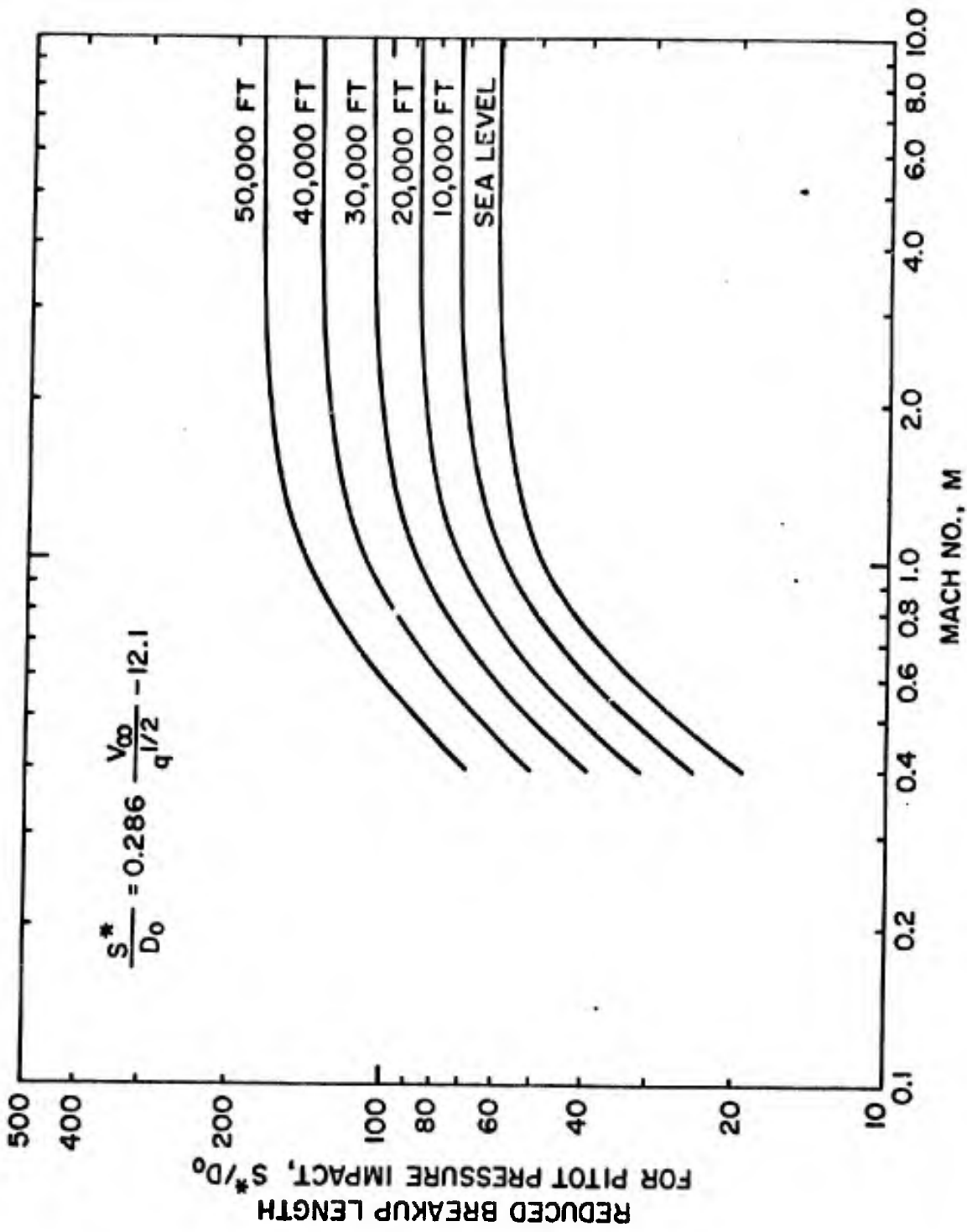


Figure 11. Normalized Drop Breakup Distance versus Mach Number

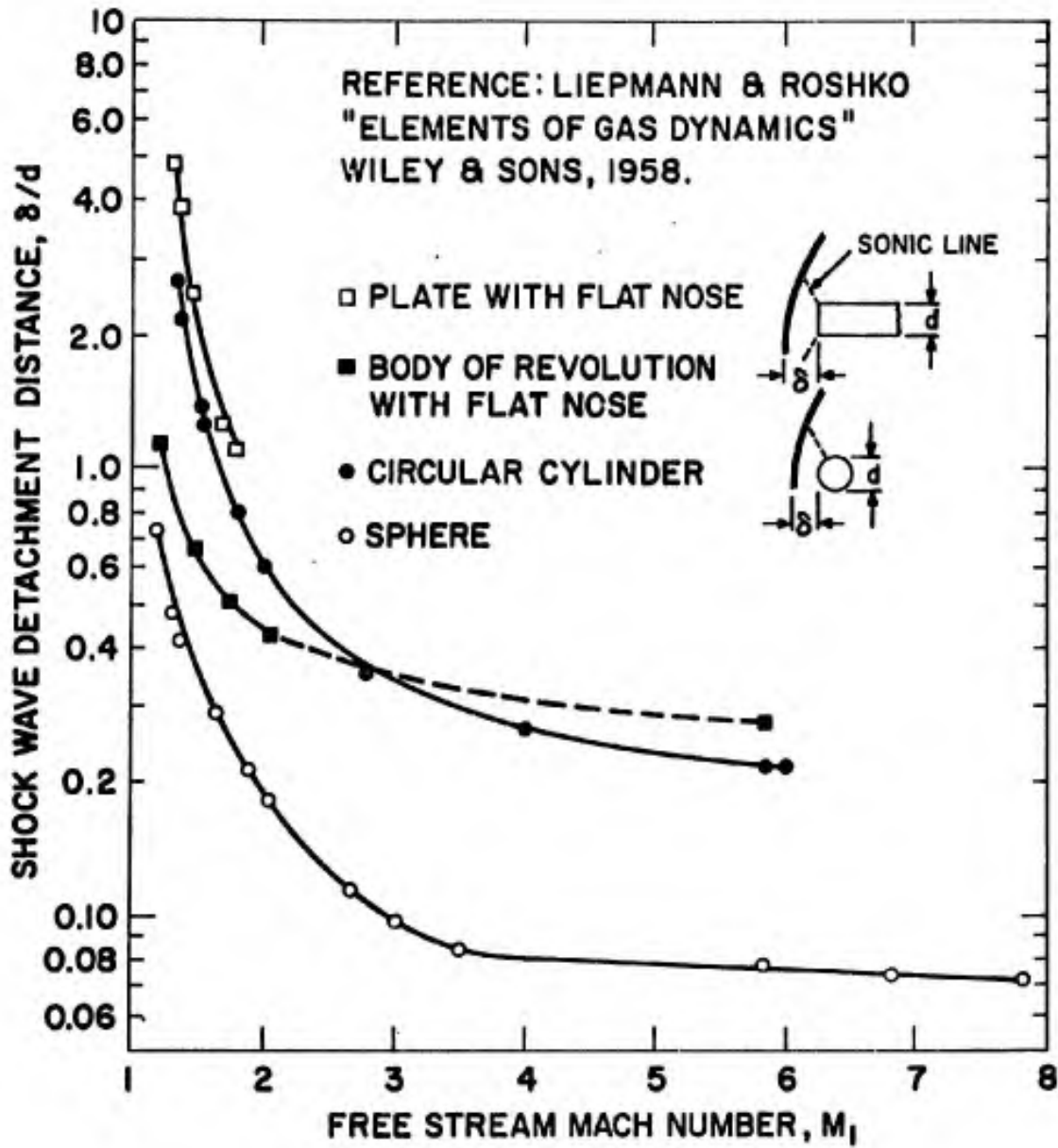


Figure 12. Blunt Body Shock Stand-Off Distance versus Mach Number

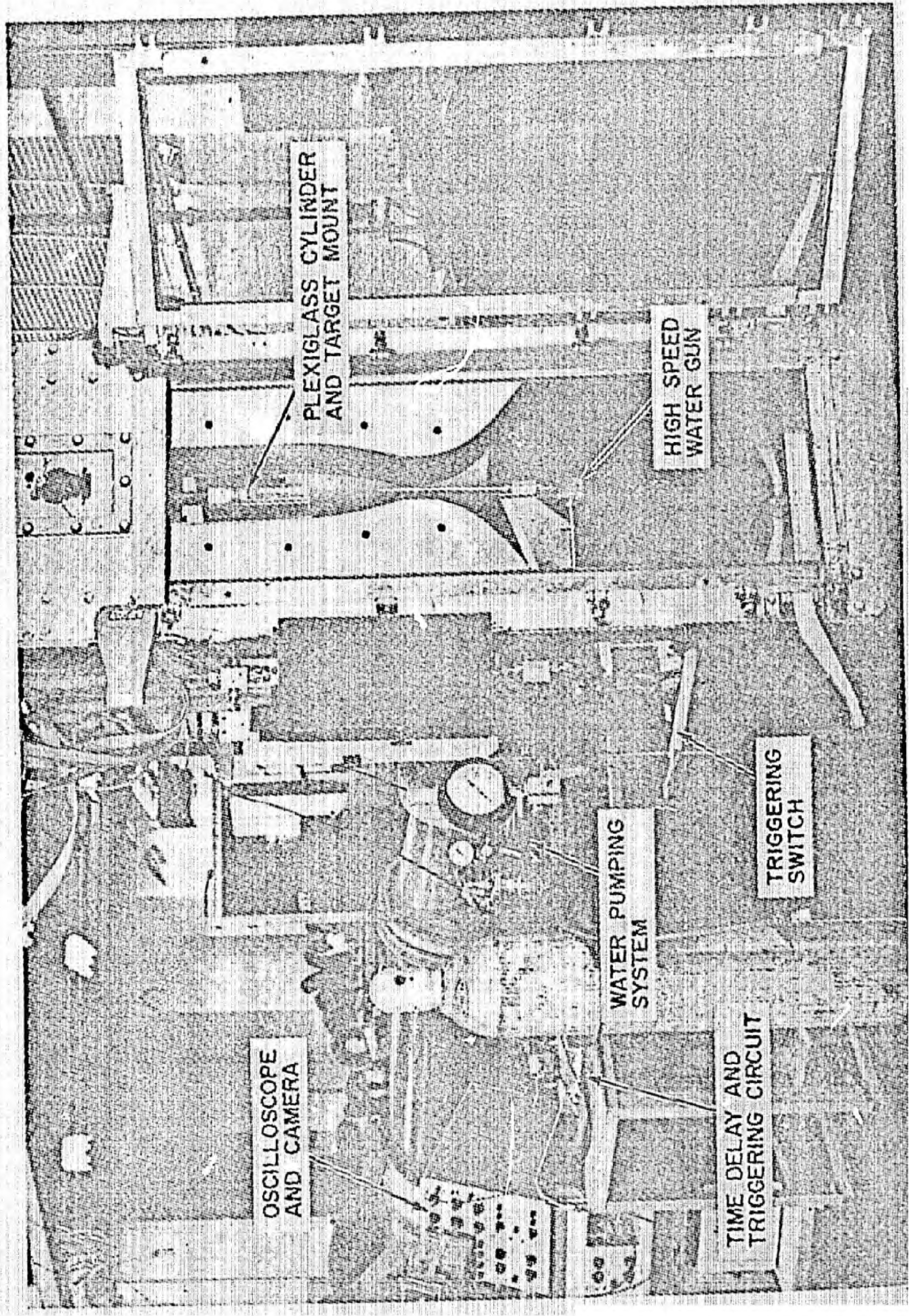


Figure 13. Wind tunnel Test Setup for Drop Breakup Studies

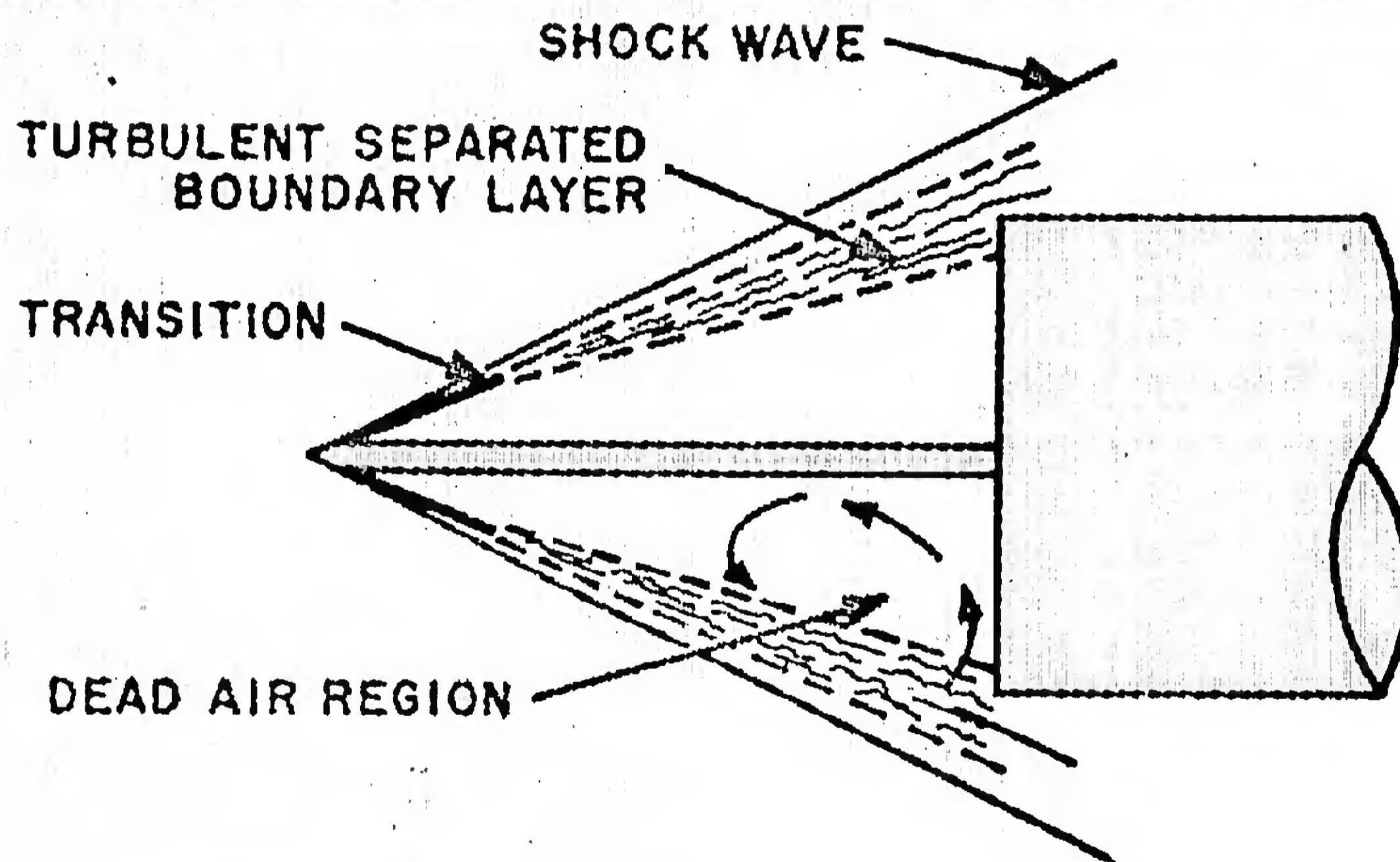
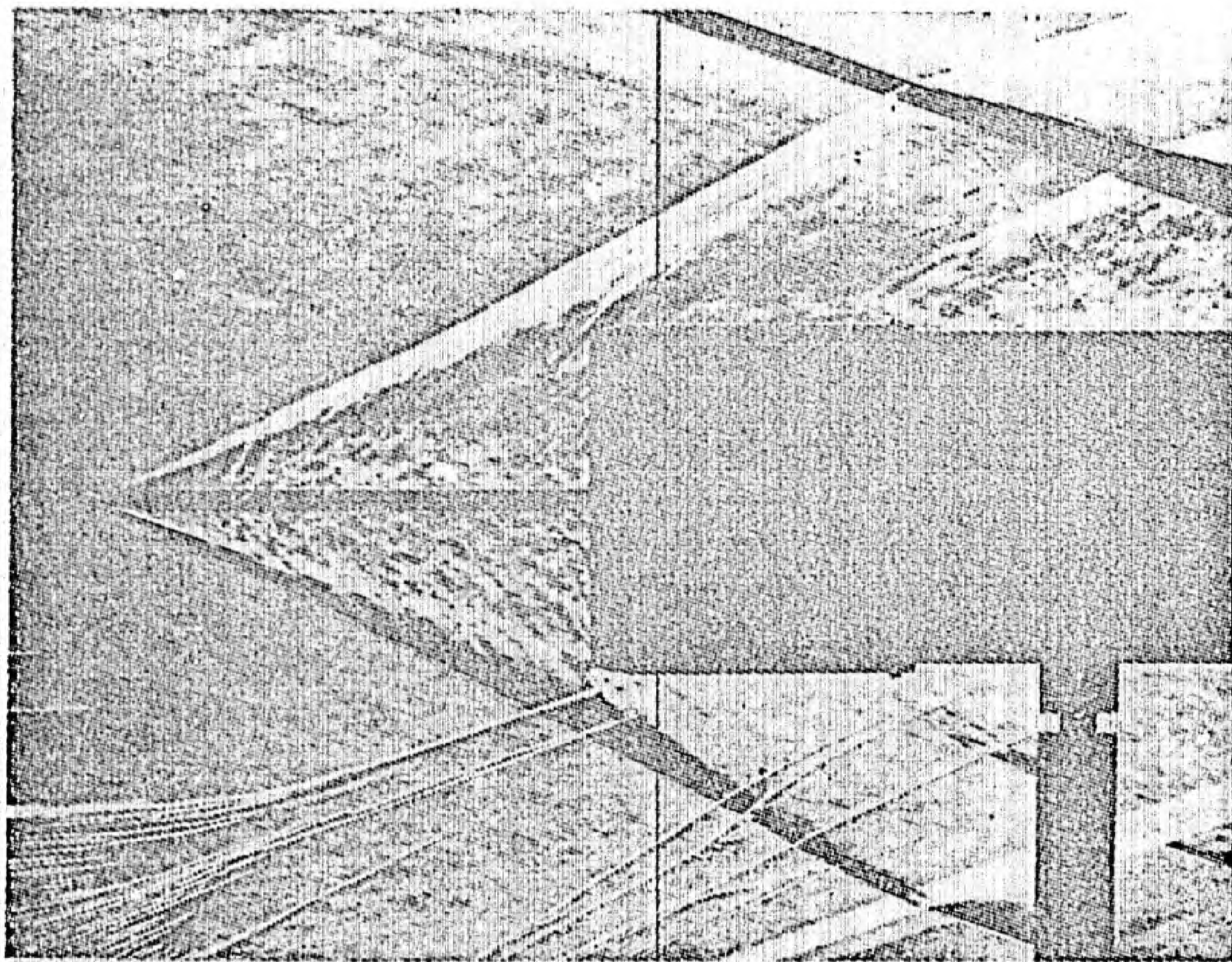


Figure 14. Spike Induced Flow Pattern in Supersonic Protected Faceplate

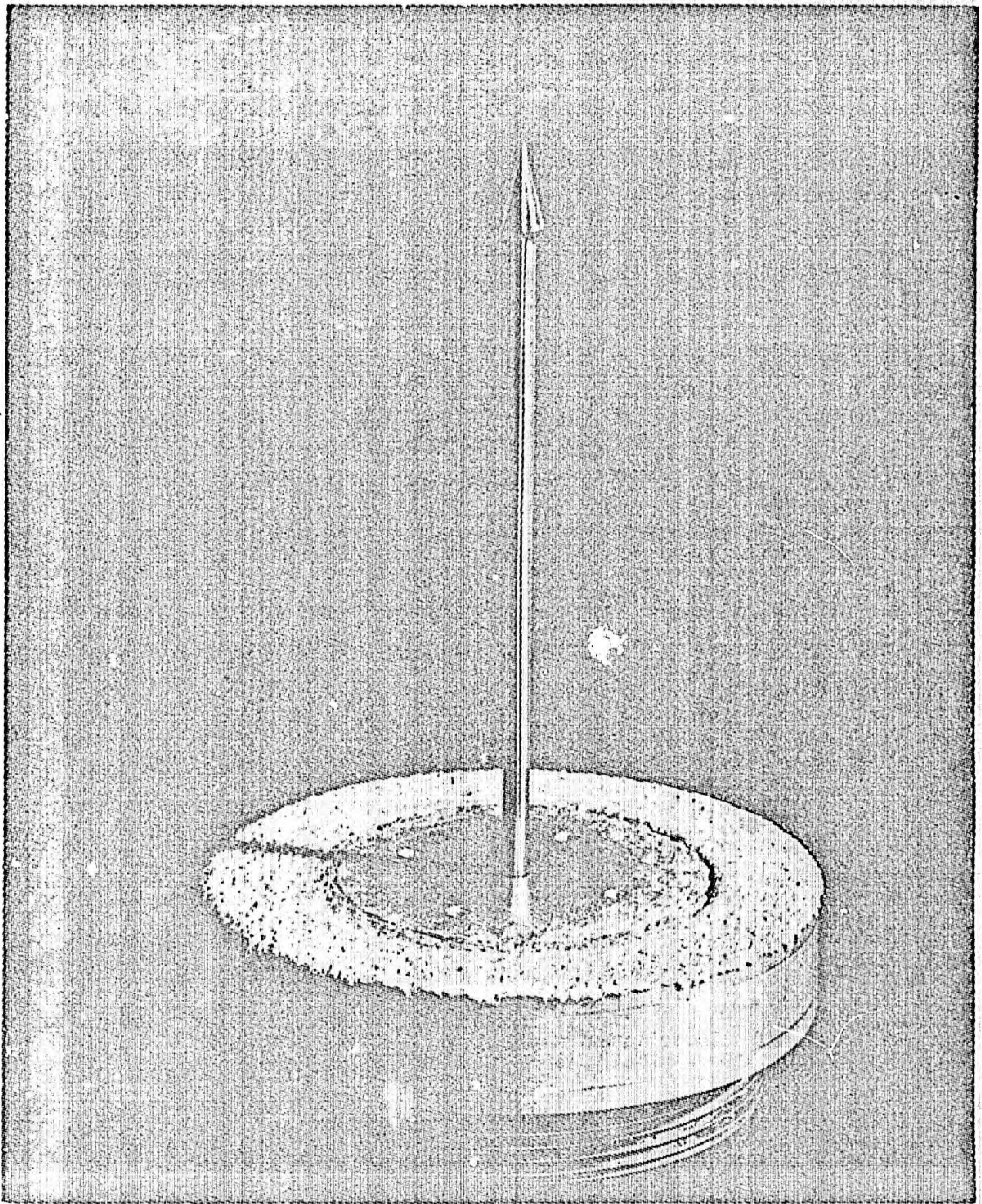


Figure 15. Post Test Photograph of Spike Protected Faceplate

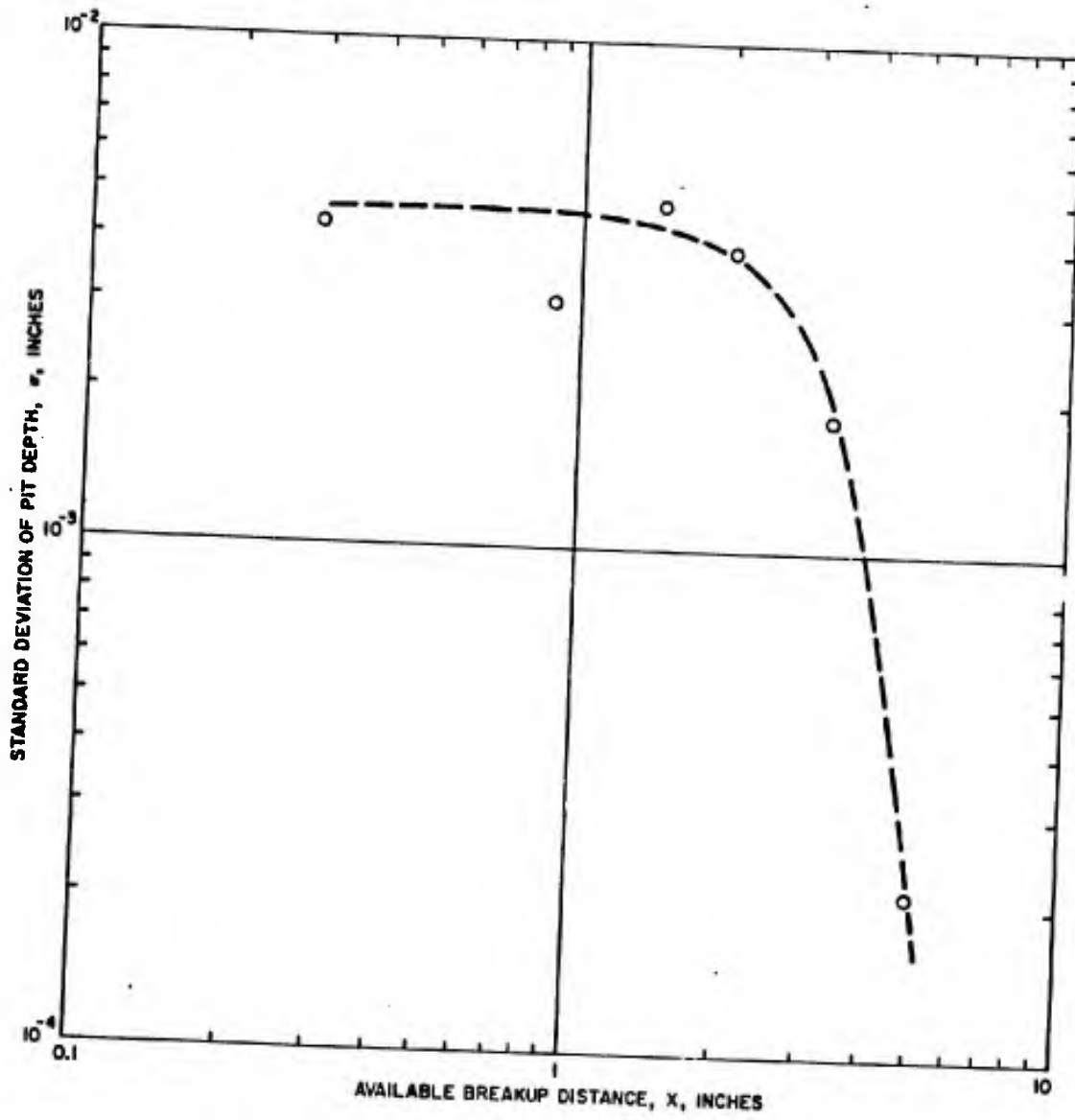


Figure 16. Distribution of Faceplate Surface Roughness

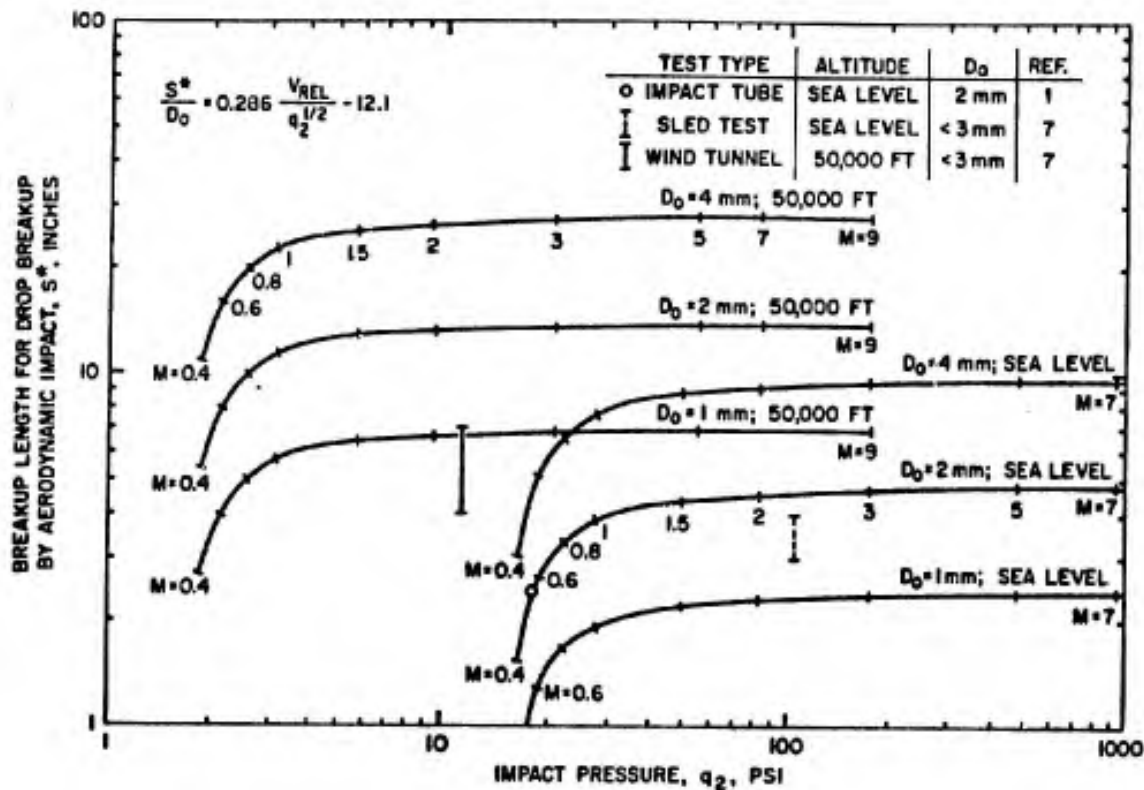


Figure 17. Distance Required to Break Up Droplets by Aerodynamic Impact